

Analysis of vibrational resonance in a quintic oscillator

S. Jeyakumari,¹ V. Chinnathambi,¹ S. Rajasekar,^{2,a)} and M. A. F. Sanjuan³

¹Department of Physics, Sri K.G.S. Arts College, Srivaikuntam, Tamilnadu 628 619, India

²School of Physics, Bharathidasan University, Tiruchirapalli, Tamilnadu 620 024, India

³Departamento de Física, Universidad Rey Juan Carlos, Tulipán s/n, Móstoles, Madrid 28933, Spain

(Received 18 August 2009; accepted 14 November 2009; published online 9 December 2009)

We consider a damped quintic oscillator with double-well and triple-well potentials driven by both low-frequency force $f \cos \omega t$ and high-frequency force $g \cos \Omega t$ with $\Omega \gg \omega$ and analyze the occurrence of vibrational resonance. The response consists of a slow motion with frequency ω and a fast motion with frequency Ω . We obtain an approximate analytical expression for the response amplitude Q at the low-frequency ω . From the analytical expression of Q , we determine the values of ω and g (denoted as ω_{VR} and g_{VR}) at which vibrational resonance occurs. The theoretical predictions are found to be in good agreement with numerical results. We show that for fixed values of the parameters of the system, as ω varies, resonance occurs at most one value of ω . When the amplitude g is varied we found two and four resonances in the system with double-well and triple-well cases, respectively. We present examples of resonance (i) without cross-well motion and (ii) with cross-well orbit far before and far after it. ω_{VR} depends on the damping strength d while g_{VR} is independent of d . Moreover, the effect of d is found to decrease the response amplitude Q .
© 2009 American Institute of Physics. [doi:10.1063/1.3272207]

The study of nonlinear systems subjected to external periodic force and noise led to several fascinating phenomena. Stochastic resonance¹ is one such phenomenon in which an enhancement of amplitude of signal is observed at an optimum noise intensity. It has been shown both theoretically and experimentally that amplification of response can be achieved when noise is replaced by a high-frequency periodic force, and the associated effect is called vibrational resonance.² The analysis of vibrational resonance has received a considerable interest in recent years because of its wide variety of applications, like the stochastic resonance, in engineering and science, deterministic in behavior and relatively easier than tuning a noise source. From both theoretical and practical standpoints, it is of great importance to obtain an analytical estimate of control parameters at which vibrational resonance occurs and analyze its features in a variety of nonlinear systems. In the present work, we report our study on vibrational resonance in a double- and a triple-well damped quintic oscillator. From the theoretical expression of the response amplitude we determine the values of the control parameters at which vibrational resonance occurs without calculating the response amplitude. The system is found to exhibit single and multiple resonances. The condition for vibrational resonance is discussed.

I. INTRODUCTION

The vibrational resonance phenomenon has been found in the double-well Duffing oscillator,²⁻⁴ spatially extended,⁵ excitable⁶ systems, an overdamped bistable system,⁷⁻⁹ and overdamped two-coupled anharmonic oscillators.^{10,11} The effects of noise on vibrational resonance have also been ana-

lyzed in certain systems.^{7,12,13} Experimental evidence of vibrational resonance was found in a bistable vertical cavity surface emitting laser¹³ and an optical system.¹⁴ In a diode laser and logistic map the high-frequency force was found to induce noise-free stochastic resonance in an intermittency region.¹⁵ In overdamped bistable systems the signal-to-noise ratio (SNR) profile in stochastic resonance and the response amplitude profile in vibrational resonance are found to be similar. In the stochastic resonance SNR is found to be maximum when there is a synchronization between the input periodic signal and the random switching events induced by the external noise. Vibrational resonance is associated with the crossing of a barrier in bistable systems with periodic switching between two states. Further, at the resonance, bifurcation of effective potential of slow motion of the system is found. It is important to investigate the mechanism of vibrational resonance in different kinds of systems and explore the possibility of obtaining an analytical expression for the values of a control parameter at which vibrational resonance occurs.

In the present work, we consider the damped quintic oscillator with double-well and triple-well potentials and analyze the occurrence of vibrational resonance. The equation of motion of the quintic oscillator driven by two periodic forces is given by

$$\ddot{x} + d\dot{x} + \omega_0^2 x + \beta x^3 + \gamma x^5 = f \cos \omega t + g \cos \Omega t, \quad (1)$$

where $\Omega \gg \omega$ and the potential of the system in the absence of damping and external force is

$$V(x) = \frac{1}{2} \omega_0^2 x^2 + \frac{1}{4} \beta x^4 + \frac{1}{6} \gamma x^6. \quad (2)$$

Recently, in the quintic oscillator, routes to chaos,¹⁶ resonant and nonresonant oscillations using multiple-scale perturbation theory,^{17,18} evolution of basin of attraction with the variation in parameters of the potential function,¹⁹ occur-

^{a)}Electronic mail: rajasekar@physics.bdu.ac.in.

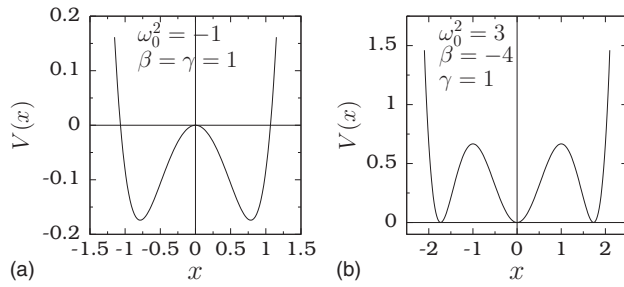


FIG. 1. (a) Double-well potential of the quintic oscillator for $\omega_0^2 < 0$, $\beta, \gamma > 0$ and (b) triple-well potential for $\omega_0^2, \gamma > 0$, $\beta < 0$, $\beta^2 > 4\omega_0^2\gamma/3$.

rence of horseshoe chaos and various bifurcation patterns,²⁰ chaotic dynamics with parametric excitation,²¹ and the effect of linear feedback and parametric perturbation on the amplitude of oscillation and chaotic escape²² have been studied. In the overdamped version of system (1) stochastic resonance²³ and splitting of Kramers escape rate²⁴ were analyzed. Pollak and Talkner²⁵ calculated Kramers rate in the triple-well case of the quintic oscillator. Rab *et al.*²⁶ studied tunneling of a dilute gas Bose–Einstein condensate in a triple-well system. The effect of time delay in the overdamped quintic oscillator in the presence of additive and multiplicative noises has been analyzed by Jia.²⁷ The occurrence of chaos has been studied in the parametrically driven triple-well system.²⁸

In the system (1) we show the occurrence of single and multiple resonances and through a theoretical approximation we determine the values of the control parameters ω , g , and Ω at which the vibrational resonance occurs. The plan of the paper is as follows. For $\Omega \gg \omega$ the solution of the system (1) consists of a slow motion $X(t)$ and a fast motion $\psi(t, \Omega t)$ with frequencies ω and Ω , respectively. We obtain the equation of motion for the slow motion and an approximate analytical expression for the response amplitude Q of the low-frequency (ω) output oscillation in Sec. II. Using this theoretical expression of Q , in Sec. III, we analyze the occurrence of vibrational resonance in the system (1) with a double-well form of the potential [Fig. 1(a)]. We obtain the analytical expressions of the control parameters ω , g , and Ω at which vibrational resonance occurs. Resonance is observed even in the absence of cross-well motion. We show that at most only one resonance occurs when the parameter ω is varied. On the other hand, when g is varied, double resonance is observed. In Sec. IV, for the triple-well case [Fig. 1(b)] we determine the intervals of ω and the values of g at which two, three, and four resonances occur and verify the theoretical prediction with numerical simulation. Finally, Sec. V contains the conclusion.

II. THEORETICAL DESCRIPTION OF VIBRATIONAL RESONANCE

For $\Omega \gg \omega$ we assume that the solution of Eq. (1) consists of a slow motion $X(t)$ with period $2\pi/\omega$ and a fast motion $\psi(t, \Omega t)$ with period $2\pi/\Omega$ (or period 2π in the fast time $\tau = \Omega t$). The mean value of the fast motion is $\psi_{av} = (1/2\pi) \int_0^{2\pi} \psi d\tau = 0$. Substituting $x = X + \psi$ in Eq. (1) we obtain the following set of equations of motion:

$$\ddot{X} + d\dot{X} + (\omega_0^2 + 3\beta\psi_{av}^2 + 5\gamma\psi_{av}^4)X + (\beta + 10\gamma\psi_{av}^2)X^3 + \gamma X^5 + \beta\psi_{av}^3 + \gamma\psi_{av}^5 = f \cos \omega t, \quad (3)$$

$$\begin{aligned} \ddot{\psi} + d\dot{\psi} + \omega_0^2\psi + 3\beta X^2(\psi - \psi_{av}) + 3\beta X(\psi^2 - \psi_{av}^2) \\ + \beta(\psi^3 - \psi_{av}^3) + 5\gamma X^4(\psi - \psi_{av}) + 10\gamma X^3(\psi^2 - \psi_{av}^2) \\ + 10\gamma X^2(\psi^3 - \psi_{av}^3) + 5\gamma X(\psi^4 - \psi_{av}^4) + \gamma(\psi^5 - \psi_{av}^5) \\ + 10\gamma X^2\psi_{av}^2 = g \cos \Omega t, \end{aligned} \quad (4)$$

where $\psi_{av}^i = (1/2\pi) \int_0^{2\pi} \psi^i d\tau$, $i = 1, 2, \dots, 5$. Because ψ is assumed to be rapidly varying we approximate Eq. (4) as $\ddot{\psi} = g \cos \Omega t$ by treating $\ddot{\psi} \gg \dot{\psi}$, ψ , ψ^2 , ψ^3 , ψ^4 , ψ^5 . We obtain $\psi = -(g/\Omega^2) \cos \Omega t$, $\psi_{av} = 0$, $\psi_{av}^2 = g^2/(2\Omega^4)$, $\psi_{av}^3 = 0$, $\psi_{av}^4 = 3g^4/(8\Omega^4)$, and $\psi_{av}^5 = 0$. Then Eq. (3) becomes

$$\ddot{X} + d\dot{X} + C_1X + C_2X^3 + \gamma X^5 = f \cos \omega t, \quad (5a)$$

where

$$C_1 = \omega_0^2 + \frac{3\beta g^2}{2\Omega^4} + \frac{15\gamma g^4}{8\Omega^8}, \quad C_2 = \beta + \frac{5\gamma g^2}{\Omega^4}. \quad (5b)$$

Equations (5a) and (5b) can be treated as the equations of motion for the slow motion of a particle in the effective potential

$$V_{\text{eff}}(X) = \frac{1}{2}C_1X^2 + \frac{1}{4}C_2X^4 + \frac{1}{6}\gamma X^6. \quad (6)$$

Comparing $V(x)$ [Eq. (2)] and the above $V_{\text{eff}}(X)$, we infer that the number of equilibrium states can be changed by varying the parameters g or Ω . The equilibrium points about which slow oscillations take place are given by

$$\begin{aligned} X_1^* = 0, \quad X_{2,3}^* = \pm \left[\frac{-C_2 + \sqrt{C_2^2 - 4C_1\gamma}}{2\gamma} \right]^{1/2}, \\ X_{4,5}^* = \pm \left[\frac{-C_2 - \sqrt{C_2^2 - 4C_1\gamma}}{2\gamma} \right]^{1/2}. \end{aligned} \quad (7)$$

$V(x)$ is (i) a double-well potential for $\omega_0^2 < 0$, $\gamma > 0$, β -arbitrary or $\omega_0^2 < 0$, $\gamma < 0$, $\beta > 0$ with $\beta^2 > 4\omega_0^2\gamma$ and (ii) a triple-well potential for $\omega_0^2 > 0$, $\gamma > 0$, $\beta < 0$ with $\beta^2 > 4\omega_0^2\gamma$. V_{eff} is (i) a double-well form for $C_1 < 0$, $\gamma > 0$, C_2 -arbitrary or $C_1 < 0$, $\gamma < 0$, $C_2 > 0$ with $C_2^2 > 4C_1\gamma$ and (ii) a triple-well potential for $C_1 > 0$, $\gamma > 0$, $C_2 < 0$ with $C_2^2 > 4C_1\gamma$. Suppose $V(x)$ is a double-well potential with $\omega_0^2 < 0$, $\gamma > 0$, $\beta > 0$ with $\beta^2 > 4\omega_0^2\gamma$, then V_{eff} is a double-well form for $C_1 < 0$, $C_2 > 0$; a single-well form for $C_1 > 0$, $C_2 > 0$ or $C_1 > 0$, $C_2 < 0$ with $C_2^2 < 4C_1\gamma$ and a triple-well potential for $C_1 > 0$, $C_2 < 0$ with $C_2^2 > 4C_1\gamma$. Consequently, by varying g or Ω the number of equilibrium points about which slow motion occurs can be changed.

We obtain the following equation for the deviation of the slow motion X from X^* by substituting $Y = X - X^*$ in Eq. (5a):

$$\ddot{Y} + d\dot{Y} + \alpha_1 Y + \alpha_2 Y^2 + \alpha_3 Y^3 + \alpha_4 Y^4 + \gamma Y^5 = f \cos \omega t, \quad (8a)$$

where

$$\alpha_1 = C_1 + 3C_2X^{*2} + 5\gamma X^{*4}, \quad \alpha_2 = 3C_2X^* + 10\gamma X^{*3}, \quad (8b)$$

$$\alpha_3 = C_2 + 10\gamma X^{*2}, \quad \alpha_4 = 5\gamma X^*. \quad (8c)$$

For $f \ll 1$ we assume that $|Y| \ll 1$ and neglect the nonlinear terms in Eq. (8a). Then in the limit $t \rightarrow \infty$, $Y(t) = A_L \cos(\omega t - \phi)$, where

$$A_L = \frac{f}{[(\omega_r^2 - \omega^2)^2 + d^2 \omega^2]^{1/2}}, \quad \phi = \tan^{-1} \left(\frac{\omega^2 - \alpha_1}{d\omega} \right). \quad (9)$$

$\omega_r = \sqrt{C_1}$ if $X^* = 0$, otherwise $\sqrt{\alpha_1}$. We define the response amplitude Q as

$$Q = \frac{A_L}{f} = \frac{1}{[(\omega_r^2 - \omega^2)^2 + d^2 \omega^2]^{1/2}}. \quad (10)$$

III. RESONANCE WITH DOUBLE-WELL POTENTIAL

In this section we analyze the vibrational resonance in the double-well potential system with $\omega_0^2 < 0$, β , and $\gamma > 0$. For $g < g_0$, where

$$g_0 = \Omega^2 \left[\frac{-\beta + \sqrt{\beta^2 + (10\gamma|\omega_0^2|/3)}}{5\gamma/2} \right]^{1/2}, \quad (11)$$

in Eq. (5), $C_1 < 0$, $C_2 > 0$, V_{eff} remains as a double-well potential, and the slow oscillations take place around $X_{2,3}^*$, while for $g > g_0$ it becomes a single-well with $C_1, C_2 > 0$ and the slow oscillation takes place around $X_1^* = 0$.

From the theoretical expression of Q we can determine the values of a control parameter at which vibrational resonance occurs. We can rewrite Eq. (10) as $Q = 1/\sqrt{S}$ where

$$S = (\omega_r^2 - \omega^2)^2 + d^2 \omega^2, \quad (12)$$

and ω_r is the natural frequency of the linear version of the equation of motion of slow motion in the absence of the external force $f \cos \omega t$. It is called resonant frequency (of the low-frequency oscillation). Moreover, ω_r is independent of f , ω , and d , and depends on other parameters ω_0^2 , β , γ , g , and Ω . When the control parameter g or ω or Ω is varied the occurrence of vibrational resonance is determined by the value of ω_r . Specifically, as the control parameter g or Ω varies, the value of ω_r also varies and a resonance occurs if the value of ω_r is such that the function S is a minimum. Thus a local minimum of S represents a resonance. By finding the minima of S , the values of g_{VR} or ω_{VR} or Ω_{VR} at which resonance occurs can be determined. For example,

$$\omega_{\text{VR}} = \sqrt{\omega_r^2 - \frac{d^2}{2}}. \quad (13)$$

For fixed values of the parameters, as ω varies from zero, the response amplitude Q becomes maximum at $\omega = \omega_{\text{VR}}$ given by Eq. (13). Resonance does not occur for the parametric choices for which $\omega_r^2 < d^2/2$. When ω is varied from zero ω_r remains constant because it is independent of ω . Therefore, resonance will take place at most one value of ω . This is the case for other forms of the potential also.

If we fix $\omega_0^2 = -1$, $\beta = \gamma = 1$, $f = 0.05$, and $\Omega = 10$, then the value of g_0 is 65.77. In Fig. 2(a) ω_{VR} versus g is plotted for three values of d . For $d = 0.5, 1$, and 1.5 resonance will not occur if $g \in [64.3, 68.6]$, $[59.3, 76.10]$, and $[49.6, 85.6]$,

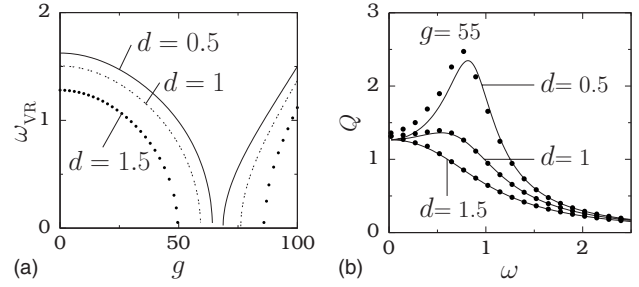


FIG. 2. (a) Plot of ω_{VR} vs g for the system (1) with a double-well potential. The values of the parameters are $\omega_0^2 = -1$, $\beta = \gamma = 1$, and $\Omega = 10$. (b) Response amplitude Q vs ω for $g = 55$ and $f = 0.05$. In the subplot (b) continuous curves are a theoretical result and the painted circles are numerically computed values of Q .

respectively. In Fig. 2(b) theoretical and numerically computed Q are plotted for $g = 55$ and for three values of d . The sine and cosine components Q_S and Q_C , respectively, are calculated from the equations

$$Q_S = \frac{2}{nT} \int_0^{nT} x(t) \sin \omega t dt, \quad (14a)$$

$$Q_C = \frac{2}{nT} \int_0^{nT} x(t) \cos \omega t dt, \quad (14b)$$

where $T = 2\pi/\omega$, and n is taken as 200. Numerically computed $Q = \sqrt{Q_S^2 + Q_C^2}/f$ is in good agreement with the theoretical approximation. In Fig. 2(b) resonance occurs for $d = 0.5$ and 1 while for $d = 1.5$ the value of Q decreases continuously when ω is varied. Both ω_{VR} and Q at the resonance decrease with increase in d .

We compare the change in the slow motion $X(t)$ and the actual motion $x(t)$. For $g = 55$, V_{eff} is also a double-well potential and $\omega_{\text{VR}} = 0.815$ for $d = 0.5$. The system (1) has two coexisting orbits and the associated slow motion takes place around the two equilibrium points $X_{2,3}^*$. This is shown in Fig. 3(a) for $\omega = 0.4, 0.75$, and 1.5 . The corresponding actual motions of the system equation (1) are shown in Figs. 3(b)–3(d). For a wide range of values of ω , including the value of ω_{VR} , $x(t)$ is not a cross-well motion, that is, it is not crossing both the equilibria $(x^*, y^*(=x^*)) = (\pm 0.786, 15, 0)$. When $g = 90$

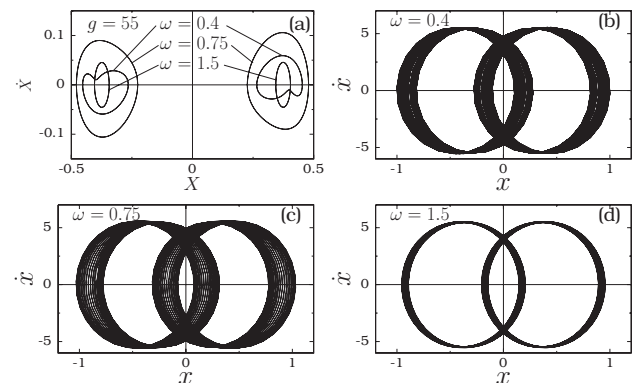


FIG. 3. Phase portraits of (a) slow motion and [(b)–(d)] actual motion of the double-well system for a few values of ω with $g = 55$ and $d = 0.5$.

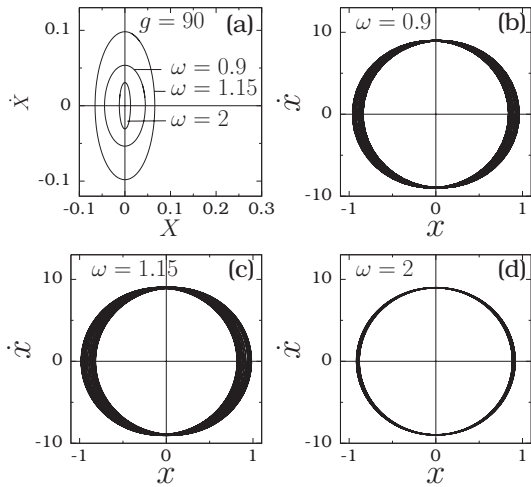


FIG. 4. Phase portraits of (a) slow motion and [(b)–(d)] actual motion of the double-well system for a few values of ω with $g=90$ and $d=0.5$.

$> g_0$, V_{eff} is a single-well potential and $\omega_{\text{VR}}=1.15$. The slow oscillations take place around $X_1^*=0$ [Fig. 4(a)] and $x(t)$ encloses both the minima ($x=\pm 0.78615$) and the local maxima ($x=0$) of the potential for all values of ω [Figs. 4(b)–4(d)].

Next, we determine g_{VR} which are roots of $S_g=dS/dg=4(\omega_r^2-\omega^2)\omega_r\omega_{rg}=0$ with $S_{gg}|_{g=g_{\text{VR}}}>0$, where $\omega_{rg}=\frac{d\omega_r}{dg}$. The variation in ω_r with g is shown in Fig. 5. From $g=g_0$ the value of ω_r monotonically increases from 0. Consequently, for a fixed value of ω there is always one resonance at a value of g at which $\omega_r^2=\omega^2$. Further, for $g>g_0$, V_{eff} is a single-well potential and $\omega_r^2=C_1$. In this case an analytical expression for g_{VR} can be easily obtained from $\omega_r^2=C_1=\omega^2$ and is given by

$$g_{\text{VR}} = \Omega^2 \left[\frac{-\beta + \sqrt{\beta^2 + (10\gamma|\omega_0^2 - \omega^2|/3)}}{5\gamma/2} \right]^{1/2}, \quad \omega^2 > \omega_0^2. \tag{15}$$

For $g < g_0$ the resonance frequency is $\sqrt{\alpha_1}$, since $C_1 < 0$. ω_r is maximum at $g=0$ and is 1.662. This implies that for $\omega > 1.662$ the function S_g never becomes 0 and, hence, resonance will not occur for any value of $g \in [0, g_0]$. For

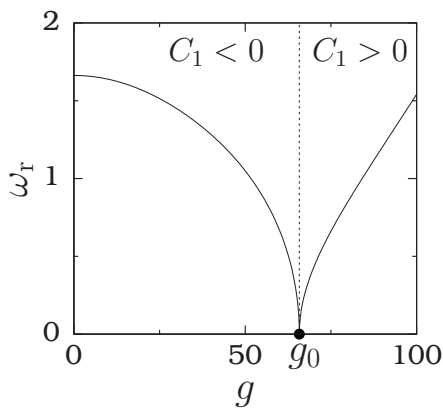


FIG. 5. ω_r vs g for the system (1) with a double-well potential.

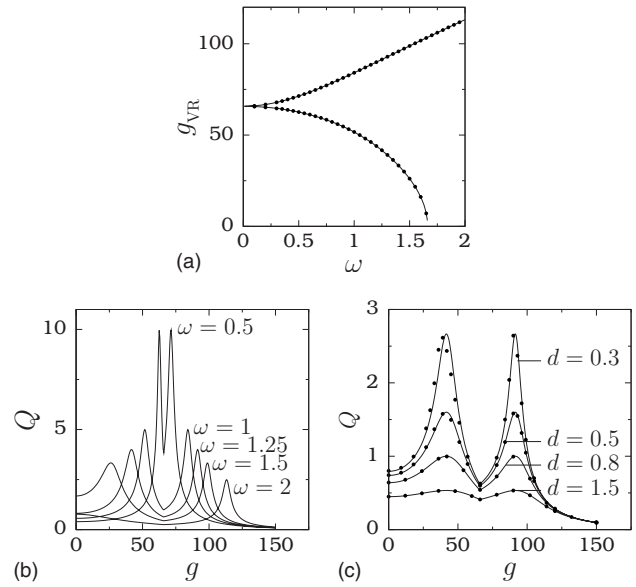


FIG. 6. (a) Plot of g_{VR} vs ω for the system (1) with a double-well potential. Theoretically and numerically calculated g_{VR} are represented by continuous curve and painted circles, respectively. (b) Theoretical response amplitude Q vs g for a few values of ω with $d=0.3$, $f=0.05$, and $\Omega=10$. (c) Q vs g for a few values of d with $\omega=1.25$. Continuous curves are a theoretical result and the painted circles are numerically computed values of Q .

$\omega < 1.662$, $S_g=0$ at a value of $g \in [0, g_0]$ so that there is a resonance. The analytical determination of the roots of $S_g=0$ and g_{VR} is difficult because C_1 , C_2 , and $X_{2,3}^*$ are functions of g , and $\omega_r^2=\alpha_1$ is a complicated function of g . Therefore, we determine the roots of $S_g=0$ and g_{VR} numerically. We analyze cases $(\omega_r^2-\omega^2)=0$ and $\omega_{rg}=0$.

In Fig. 6(a) g_{VR} computed for a range ω is plotted. For $\omega < 1.662$ there are two resonances—one at a value of $g < g_0 (=65.77)$ and another at a value of $g > g_0$, while for $\omega > 1.662$ only one resonance at a value of $g > g_0$. The above theoretical prediction is confirmed by the numerical simulation. Figure 6(b) shows the theoretical response amplitude Q as a function of g for a few values of ω . For small values of ω the two g_{VR} values are close to $g_0=65.77$. As ω increases the values of g_{VR} move away from g_0 . For $\omega=2$ we notice only one resonance. In the double-resonance cases the two resonances are almost at equidistance from g_0 and the values of Q at these resonances are the same. However, the response curve is not symmetrical about g_0 . Figure 6(c) illustrates the effect of damping on resonance. g_{VR} is unchanged by the damping strength because S_g is independent of d . However, Q at the resonance decreases with increase in d .

We note that in overdamped bistable systems^{7,9,13} $Q=1/\sqrt{\omega_r^2+\omega^2}$, g_{VR} is independent of ω and resonance occurs when the effective potential undergoes transition from a double-well form to a single-well form. In contrast to this, in the damped system (1), g_{VR} depends on ω and resonance without bifurcation of V_{eff} is found. The mechanism of vibrational resonance in overdamped systems is a minimization of the resonant frequency ω_r . In the underdamped quintic oscillator, when g is varied, the mechanism is locally minimizing $(\omega_r^2-\omega^2)$. This happens when either the resonant frequency is tuned to match with the low-frequency ω of the

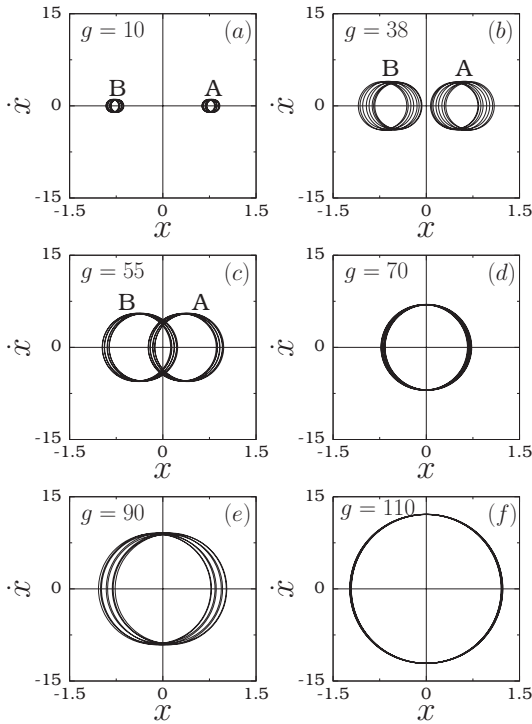


FIG. 7. Phase portrait of actual motion of the double-well system for a few values of g around the two resonances with $d=0.3$ and $\omega=1.25$. A and B are two coexisting orbits.

input signal or $\omega_{rg}=0$ with $S_{gg}>0$. The former is the case realized in the examples shown in Figs. 5 and 6. [The latter is found in the triple-well case of the system (1) and is pointed out in Sec. IV.] When ω is varied the resonant frequency is unaltered and the mechanism is a minimization of S given by Eq. (12).

We now study the nature of the solution $x(t)$ near the two resonances at $g=38.61$ and 90.59 for $d=0.3$ and $\omega=1.25$, shown in Fig. 6(c). Figure 7 shows the phase portrait of actual motion for several values of g . For $g < g_0=65.77$ the system (1) has two coexisting orbits. As g increases from a small value, the size of the two orbits increases and the equilibrium points $X_{2,3}^*$, about which the corresponding slow motions take place, move toward the origin. This is shown in Fig. 7 for $g=10$ and 38 . For $g > g_0$ the actual motion (as well as the slow motion) occurs around the origin. This is shown for $g=90$ and 110 . The resonance at $g=38.61$ occurs without a cross-well motion. On the other hand, $x(t)$ is a cross-well orbit far before and far after the resonance at $g=90.59$.

We calculated the mean residence time τ_{MR} of $x(t)$, the average time spent by the trajectory in a well before switching to another well, in the left well and right well. As shown in Fig. 7 two orbits coexist for $g < g_0=65.77$. For small values of g , one orbit is confined to the left well while the other is confined to the right well. For the starting value of g , we have chosen the orbit completely lying in the region $x > 0$. In the calculation of τ_{MR} averaging is performed for 500 initial conditions and over 1000 drive cycles of the low-frequency force, after leaving sufficient transient motion. For $g < g_c=41.6$ the size of the orbit increases when the value of g increases; however, the orbit remains in the region $x > 0$.

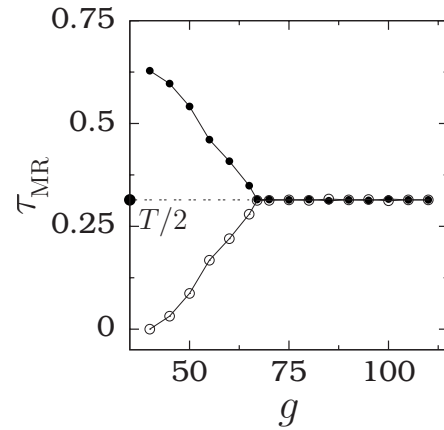


FIG. 8. Variation in numerically calculated mean residence time τ_{MR} of $x(t)$ in the right well (represented by painted circles) and in the left well (represented by open circles) with the parameter g . $g_{g_{VR}}=38.61$ and 90.59 .

Thus, for $g < g_c$, τ_{MR}^R (mean residence time in the right well) is infinite and τ_{MR}^L (mean residence time in the left well) is zero. Figure 8 shows the plot of τ_{MR} in the two wells for $g > g_c$. As g increases further from g_c , the orbit visits the region $x < 0$, but the orbit is not symmetric about the origin. This is because slow oscillation takes place about the equilibrium point $X_2^* \neq 0$. We can clearly notice this for the orbit A in Fig. 7(c) where $g=55$. Due to the asymmetry of the orbit, τ_{MR}^R and τ_{MR}^L are different. The equilibrium point X_2^* (as well as X_3^*) moves toward the origin with g , and the orbit visits more the region in the left well. Consequently, τ_{MR} in the right well decreases with increase in g , while it increases in the left well. For $g > g_0=65.77$, V_{eff} becomes a single-well and slow motion is about the origin. τ_{MR} in the two wells are equal because the actual motion of the system (1) is now symmetric about the origin. The point is that far before the resonance ($g=90.59$), τ_{MR} in the two wells are equal and are $T/2$, where $T=2\pi/\Omega$ is the period of the high-frequency force. In the stochastic resonance case, at resonance τ_{MR} in the two wells is $T/2$ and after resonance it decreases with increase in the noise intensity.

Resonance can be observed by varying also the frequency Ω of the high-frequency force $g \cos \Omega t$. Ω_{VR} are roots of $S_{\Omega} = dS/d\Omega = 4(\omega_r^2 - \omega^2)\omega_r\omega_{r\Omega} = 0$ with $S_{\Omega\Omega}|_{\Omega=\Omega_{VR}} > 0$, where $\omega_{r\Omega} = d\omega_r/d\Omega$. Further, for $\Omega < \Omega_0$ given by

$$\Omega_0 = \left[\frac{5\gamma g^2/2}{-\beta + \sqrt{\beta^2 + (10\gamma|\omega_0^2|/3)}} \right]^{1/4}, \quad (16)$$

V_{eff} becomes a single-well potential with $\omega_r^2 = C_1$ and we obtain

$$\Omega_{VR} = \left[\frac{5\gamma g^2/2}{-\beta + \sqrt{\beta^2 + (10\gamma|\omega_0^2 - \omega^2|/3)}} \right]^{1/4}, \quad \omega^2 > \omega_0^2. \quad (17)$$

For $\Omega > \Omega_0$, V_{eff} is a double-well form with $\omega_r^2 = \alpha_1$ and the analytical expression for Ω_{VR} is difficult to find as in the case of $g < g_0$.

TABLE I. Nature of the effective potential V_{eff} and the sign of C_1 and C_2 for various ranges of g/Ω^2 for $\omega_0^2=3$, $\beta=-4$ and $\gamma=1$.

Range of g/Ω^2	Sign of C_1 and C_2	Type of V_{eff}
$0 < g/\Omega^2 < 0.7876$	$C_1 > 0, C_2 < 0, C_2^2 > 4C_1\gamma$	Triple-well
$0.7876 < g/\Omega^2 < 0.8945$	$C_1, C_2 < 0$	Double-well
$0.8945 < g/\Omega^2 < 1.6061$	$C_1 < 0, C_2 > 0$	Double-well
$g/\Omega^2 > 1.6061$	$C_1, C_2 > 0$	Single-well

IV. RESONANCE WITH A TRIPLE-WELL POTENTIAL

The potential of the system (1) has three wells for ω_0^2 , $\gamma > 0$, $\beta < 0$, and $\beta^2 > 4\omega_0^2\gamma/3$. We fix $\omega_0^2=3$, $\beta=-4$, and $\gamma=1$. In contrast to the double-well case, in the triple-well case the signs of both C_1 and C_2 in Eq. (5b) can be changed by varying the parameters g or Ω . Consequently, the shape of the effective potential changes from triple-well to double-well and single-well, as indicated in Table I.

In the triple-well potential, also for fixed values of g and d , the value of ω at which resonance occurs is given by Eq. (13). When V_{eff} becomes a triple-well form slow oscillations take place around $X_1^*=0$ and $X_{4,5}^*$. Figure 9(a) shows the variation in ω_{VR} with g for $\Omega=10$ and for three values of d , where slow motions around $X_{4,5}^*$ are considered for the triple-well form of V_{eff} . For a fixed value of g , ω_{VR} decreases with increase in d . For $d=2.5$ and $g \in [54.02, 99.54]$ and $[141.33, 179.44]$, resonance does not occur when ω is varied because

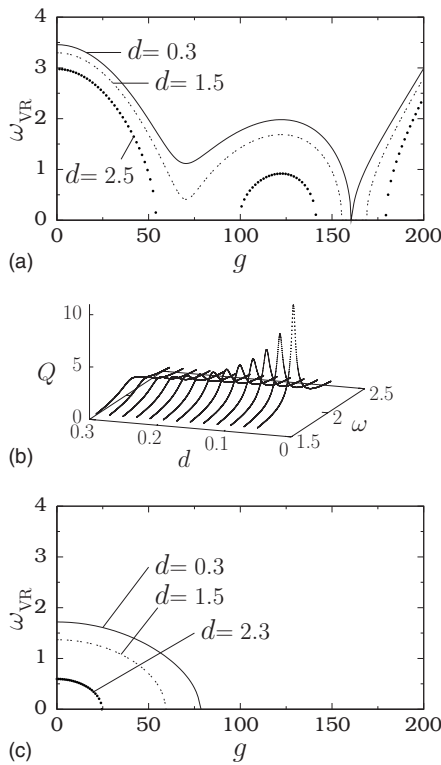


FIG. 9. (a) ω_{VR} vs g for the system (1) with triple-well potential. The associated slow motions are around $X_{4,5}^*$. The values of the parameters are $\omega_0^2=3$, $\beta=-4$, $\gamma=1$, and $\Omega=10$. (b) Variation in Q with ω for $g=125$, $f=0.05$ and for several values of d . (c) ω_{VR} vs g for the slow motion around $X_1^*=0$.

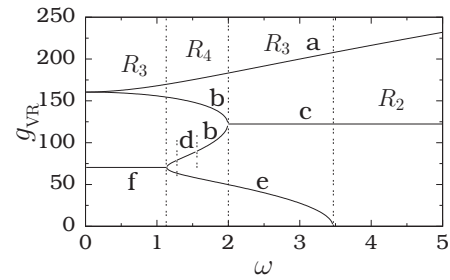


FIG. 10. Plot of g_{VR} vs ω for the system (1) with the triple-well potential. The values of the parameters are $\omega_0^2=3$, $\beta=-4$, $\gamma=1$, and $\Omega=10$. g_{VR} is independent of d . Two, three, and four resonances occur in the intervals of ω marked as R_2 , R_3 , and R_4 , respectively. For more details see the text.

$\omega_r^2 - d^2/2 < 0$ in the above regions of g . Figure 9(b) shows Q versus ω for several values of d where $g=125$. As d increases the value of Q at resonance decreases. For $g < 78.76$, in addition to the two slow motions around $X_{4,5}^*$, there is also another slow motion around $X_1^*=0$. ω_{VR} versus g for this orbit is shown in Fig. 9(c). For $d=2.5$ resonance with this orbit does not occur when ω is varied.

Next, we analyze the occurrence of resonance as g is varied. For $g > g_0=160.60$ the analytical expression for g_{VR} is given by Eq. (15), with $|\omega_0^2 - \omega^2|$ replaced by $|\omega_0^2| + \omega^2$, and the restriction $\omega^2 > \omega_0^2$ is not required. For $g < g_0$ the resonance frequency $\omega_r = \sqrt{\alpha_1}$ (we consider the orbits around $X_{4,5}^*$ in the case of a triple-well form of V_{eff}) is a complicated function of g and, hence, we determined g_{VR} numerically from Eq. (12). Figure 10 depicts g_{VR} versus ω . Curves a–f are obtained from the following cases:

- Curve a: $C_1 < 0, C_2 > 0$. g_{VR} is given by Eq. (15) with $|\omega_0^2 - \omega^2|$ replaced by $|\omega_0^2| + \omega^2$;
- Curve b: $C_1 < 0, C_2 > 0$, and $\omega_r^2 - \omega^2 = 0$;
- Curve c: $C_1 < 0, C_2 > 0$, and $\omega_{\text{rg}} = 0$;
- Curve d: $C_1 < 0, C_2 < 0$ and $\omega_r^2 - \omega^2 = 0$;
- Curve e: $C_1 > 0, C_2 < 0, C_2^2 > 4c_1\gamma$, and $\omega_r^2 - \omega^2 = 0$;
- Curve f: $C_1 > 0, C_2 < 0$, and $\omega_{\text{rg}} = 0$.

We point out that a resonance with $\omega_{\text{rg}}=0$ is not possible in the double-well Duffing oscillator [Eq. (1) with $\omega_0^2 < 0$, $\beta > 0$, and $\gamma=0$]. The various curves in Fig. 10 can be understood from the plots of ω_r and ω_{rg} versus g (Fig. 11). From Fig. 11 we infer the following:

- As in the double-well case in the triple-well system, also as g increases beyond g_0 , the value of ω_r continuously increases from 0, and thus there must be one (and only one) resonance at a value of g greater than g_0 . The resulting g_{VR} is the curve a in Fig. 10.
- The plot of ω_r has a local minimum at $g=g_2=70.4$ and a local maximum at $g=g_3=122.4$. $\omega_{\text{rg}}=0$ at these two values of g . The calculation of S_{gg} indicates that Q is maximum at g_2 for $\omega < \omega_{r1}=1.137$ and at g_3 for $\omega > \omega_{r2}=2.02$. Curves f and c represent these two values of g .
- For $0 < \omega < \omega_{r1}=1.137$ there are three resonances. First resonance occurs at $g=g_2$ due to $\omega_{\text{rg}}=0$. Second and third resonances occur in the intervals $[g_4, g_0]$ and $[g_0, g_5]$, respectively, due to $\omega_r^2 - \omega^2 = 0$. In Fig. 12(a)

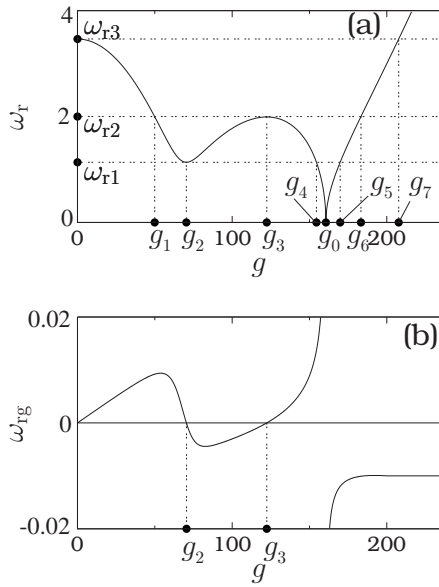


FIG. 11. Variation in (a) the resonant frequency ω_r and (b) ω_{rg} with the control parameter g for the system (1) with the triple-well potential. $\omega_{rg}=0$ at $g=70.4$ and 122.4 .

- for $\omega=1$, as g is varied, resonance occurs at $g=70.4$, 156 , and 168 .
- (iv) For $\omega_{r1} < \omega < \omega_{r2}=2$, $\omega_r = \omega$ at four values of g , one in each of the intervals $[g_1, g_2]$, $[g_2, g_3]$, $[g_3, g_4]$, and $[g_5, g_6]$. An example of four resonances is shown in Fig. 12(a) for $\omega=1.25$.
- (v) For $\omega_{r2} < \omega < \omega_{r3}=3.464$, in addition to the resonance at $g_3=122.4$, two more resonances occur—one in the interval $[0, g_1]$ and another in the interval $[g_6, g_7]$. An example is shown in Fig. 12(b) with $\omega=2$.
- (vi) For $\omega > \omega_{r3}$ two resonances occur—one at $g=g_3$ and another at a value of $g > g_7$. In Fig. 12(b) for $\omega=5$, the resonance at $g_3=122.4$ is too weak and not visible in the scale used.

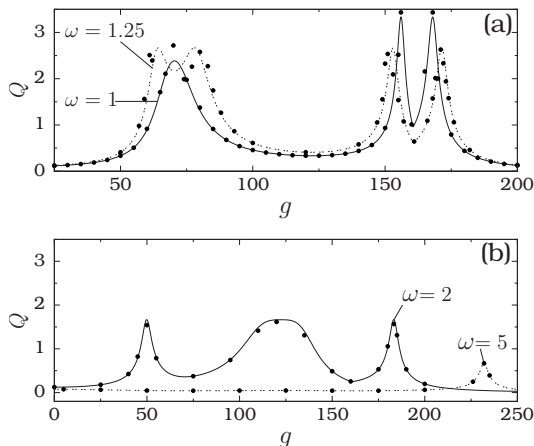


FIG. 12. Q vs g for the triple-well case for four values of ω with $d=0.3$, $\Omega=10$, and $f=0.05$. Continuous curves are theoretical Q while the painted circles are the numerically calculated Q .

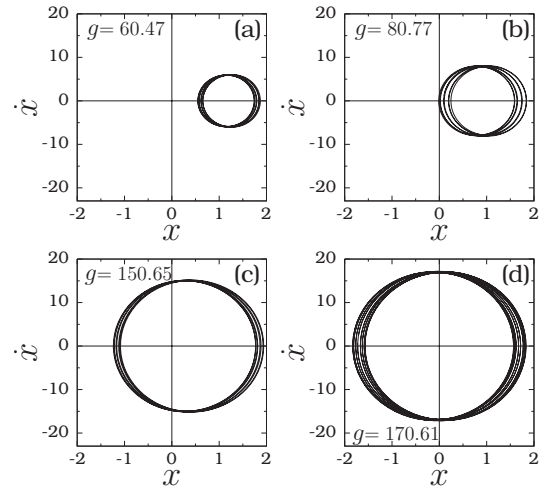


FIG. 13. Phase portrait of the actual orbits of the triple-well system at four resonances with $\omega=1.25$, $d=0.3$, $f=0.05$, and $\Omega=10$. The coexisting attractors are not shown for clarity.

For $\omega=1.25$, $d=0.3$ four resonances occur at $g=60.47$, 80.77 , 150.65 , and 170.61 . For $g > g_0=160.6$ the slow oscillation takes place around the origin, while for other values of g the center of the orbit moves toward the origin as g increases toward g_0 . Figure 13 shows the phase portrait of the actual motion of the system at four resonances. The triple-well potential has three minima at $x = \pm 1.732 05$, 0 and two maxima at $x = \pm 1$. In Fig. 13(a) at $g=g_{VR}=60.47$ $x(t)$ crosses the right-well local minimum and not crosses the middle-well minimum. For g values around $g=g_{VR}=150.65$ $x(t)$ encloses the minima of the right wells and middle wells but not crosses the left-well minimum [Fig. 13(c)]. Figure 14 shows the variation in mean residence time τ_{MR} of $x(t)$ in the three wells. At four resonances τ_{MR} of the three wells are not identical.

V. CONCLUSION

We have analyzed the occurrence of vibrational resonance in the quintic oscillator with double-well and triple-well forms of the potential. The effective potential of the system allowed us to obtain an approximate theoretical expression for the response amplitude Q at the low-frequency ω . From the analytical expression of Q we determined the values of ω and g at which vibrational resonance occurs. In

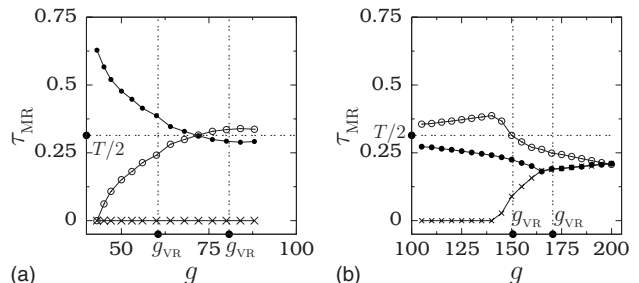


FIG. 14. Mean residence time τ_{MR} in the three wells of the triple-well system vs g . τ_{MR} of $x(t)$ in the left, middle, and right wells are represented by the painted circles, open circles, and “ \times ,” respectively.

the double-well and triple-well cases when ω is varied, we found either no resonance or only one resonance depending on the values of the other parameters of the system. As g is varied we have the following results. (i) In the double-well system there is always one resonance at a value of g , $g > g_0$, while another resonance occurs below g_0 for a range of values of ω , where g_0 is given by Eq. (11). (ii) In the system (1) with three wells also for $g > g_0$, there is always one resonance, while for $g < g_0$ one or two or three resonances occur depending on the value of ω . In the multiple-resonance case the resonant frequency is a nonmonotonically varying function of the control parameter. In all the examples considered in this paper the onset of cross-well motion is found to be not a precursor for vibrational resonance. Further, at resonance, τ_{MR} of $x(t)$ in the wells are not equal.

ACKNOWLEDGMENTS

The work of S.R. forms part of the Department of Science and Technology, Government of India sponsored research project. M.A.F.S. acknowledges the financial support from the Spanish Ministry of Education and Science under Project No. FIS2006-08525 and from the Spanish Ministry of Science and Innovation under Project No. FIS2009-09898. The authors are thankful to the referees for their suggestions which improved the presentation of this paper.

¹L. Gammaitoni, P. Hanggi, P. Jung, and F. Marchesoni, *Rev. Mod. Phys.* **70**, 223 (1998).

²P. S. Landa and P. V. E. McClintock, *J. Phys. A* **33**, L433 (2000).

³M. Gitterman, *J. Phys. A* **34**, L355 (2001).

⁴I. I. Blekhman and P. S. Landa, *Int. J. Non-Linear Mech.* **39**, 421 (2004).

⁵A. A. Zaikin, L. Lopez, J. P. Baltanas, J. Kurths, and M. A. F. Sanjuan, *Phys. Rev. E* **66**, 011106 (2002).

⁶E. Ullner, A. Zaikin, J. Garcia-Ojalvo, R. Bascones, and J. Kurths, *Phys. Lett. A* **312**, 348 (2003).

⁷J. P. Baltanas, L. Lopez, I. I. Blechman, P. S. Landa, A. Zaikin, J. Kurths, and M. A. F. Sanjuan, *Phys. Rev. E* **67**, 066119 (2003).

⁸V. N. Chizhevsky and G. Giacomelli, *Phys. Rev. E* **70**, 062101 (2004).

⁹V. N. Chizhevsky, *Int. J. Bifurcation Chaos Appl. Sci. Eng.* **18**, 1767 (2008).

¹⁰V. M. Gandhimathi, S. Rajasekar, and J. Kurths, *Phys. Lett. A* **360**, 279 (2006).

¹¹V. M. Gandhimathi, S. Rajasekar, and J. Kurths, *Int. J. Bifurcation Chaos Appl. Sci. Eng.* **18**, 2073 (2008).

¹²J. Casado-Pascual and J. P. Baltanas, *Phys. Rev. E* **69**, 046108 (2004).

¹³V. N. Chizhevsky and G. Giacomelli, *Phys. Rev. A* **71**, 011801(R) (2005).

¹⁴V. N. Chizhevsky, E. Smeu, and G. Giacomelli, *Phys. Rev. Lett.* **91**, 220602 (2003).

¹⁵T. Jüingling, H. Benner, T. Stemler, and W. Just, *Phys. Rev. E* **77**, 036216 (2008).

¹⁶J. Yu, R. Zhang, W. Pan, and L. Schimansky-Geier, *Phys. Scr.* **78**, 025003 (2008).

¹⁷R. Tchoukuegno, B. R. Nana Nbandjo, and P. Wofo, *Physica A* **304**, 362 (2002).

¹⁸M. Siewe, F. M. Moukam Kakmeni, and C. Tchawoua, *Chaos, Solitons Fractals* **21**, 841 (2004).

¹⁹A. Yu Kuznetsova, A. P. Kuznetsov, C. Knudsen, and E. Mosekilde, *Int. J. Bifurcation Chaos Appl. Sci. Eng.* **14**, 1241 (2004).

²⁰Z. Jing, Z. Yang, and T. Jiang, *Chaos, Solitons Fractals* **27**, 722 (2006).

²¹M. Siewe, F. M. Moukam Kakmeni, C. Tchawoua, and P. Wofo, *Physica A* **357**, 383 (2005).

²²R. Tchoukuegno, B. R. Nana Nbandjo, and P. Wofo, *Int. J. Non-Linear Mech.* **38**, 531 (2003).

²³F. So and K. Liu, *Physica A* **303**, 79 (2002).

²⁴P. K. Ghosh, B. C. Bag, and D. S. Ray, *Phys. Rev. E* **75**, 032101 (2007).

²⁵E. Pollak and P. Talkner, *Acta Phys. Pol. B* **32**, 361 (2001).

²⁶M. Rab, J. H. Cole, N. G. Parker, A. D. Greentree, L. C. L. Hollenberg, and A. M. Martini, *Phys. Rev. A* **77**, 061602 (2008).

²⁷Z. L. Jia, *Int. J. Theor. Phys.* **48**, 226 (2009).

²⁸M. Siewe, H. Cao, and M. A. F. Sanjuan, *Chaos, Solitons Fractals* **41**, 772 (2009).